View metadata, citation and similar papers at core.ac.uk
brought to you by CORE
provided by Elsevier - Publisher Connector

are to the first daily CBCT and the planning CT. Water equivalent path lengths and doses to the PTVs using a 3D gamma analysis were analyzed. Additional phantom experiments were conducted to evaluate mild deformations simulating weight gain/loss and rectal filling/draining. **Results:** For the phantom tests, uncorrected CBCT reconstructions had the largest HU value differences compared to the reference CT while the a priori scatter corrected CBCT reconstruction had the most accurate HU values. Regarding WEPL, the uncorrected CBCT had average of errors of 5-13 mm depending upon the phantom size and herterogeneities. A uniform scatter corrected CBCT had average range error of 3-22 mm and the a priori scatter corrected CBCT had average range errors of 1-3 mm (See Table). All WEPL errors were calculated using the refence CT of the phantoms. Doses were calculated in the same phantoms using targets simulating realistic clinical scenarios and beam combinations routinely used in the clinic. Gamma pass rates for 2%/2mm and 3%/3mm were always highest for the a priori scatter corrected CBCT at 96% and 99%, respectively. For uniform corrected CBCT dose calculations, the gamma pass rates were 78% (2%/2mm) and 86% (3%/3mm) with the worst cases being in the thorax due to an overestimation of the uniform scatter model with less attenuation and scatter in the lung. Patient doses were calculated with similar gamma pass rates but gamma rates varied more due to the realistic presence of patient daily variations of shape, target position and deformation of internal anatomy (see Figure for Prostate Example).

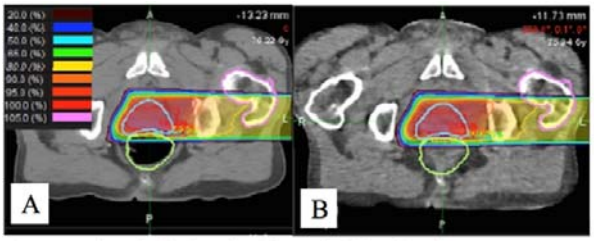

A prostate plan calculated on the reference CT (A) and on the *a priori* scatter corrected CBCT (B). The variation in the dose range is less than 2 mm.

Conclusions: Daily CBCT can be used for daily proton dose and range calculations for adaptive proton therapy when using an a priori scatter correction method. WEPL errors have been reduced from 13 mm to 3 mm and dose calculations can be performed with gamma 2%/2mm errors of less than 4%. Deformations due to weight gain/loss and target motion can be assessed with the proposed reconstruction methods. Further refinements in the CBCT reconstruction accounting for beam hardening and HU calibration specificity can reduce the range error below 3 mm.

Poster: Physics track: Imaging: focus on clinical applications

PO-0949

Advantages and shortcomings of planning hypofractionated lung treatments with VMAT on the average CT

L. Marrazzo[1], M. Casati[1], S. Pallotta[2], L. Reversi[2], P. Bonomo[3], G. Simontacchi[3], L. Livi[4], M. Bucciolini[2]
[1]*Azienda Ospedaliero-Universitaria Careggi, Medical Radiation Physics, Firenze, Italy*
[2]*University of Florence, Medical Radiation Physics, Firenze, Italy*
[3]*Azienda Ospedaliero-Universitaria Careggi, Radiation Oncology Unit, Firenze, Italy*
[4]*University of Florence, Radiation Oncology Unit, Firenze, Italy*

Purpose/Objective: A concern with the use of VMAT in hypofractionated lung treatments is whether tumour motion will lead to significant discrepancies between calculated and planned dose distributions. Our study aimed at:
a) Evaluating whether planning on the average CT scan (AVG CT) allows for a good representation of the dose distribution delivered to the moving target when 'interplay' is not considered;
b) Quantifying the interplay effect between tumour motion and dose delivery using a moving phantom and GafChromic EBT3 films.

Materials and Methods:

Patients

For ten patients who received lung treatment (54 Gy in 3 fractions), VMAT plans generated with Monaco TPS on the AVG CT were recalculated on each phase of the 4DCT and the resulting plans were compared. A Philips BigBore CT scanner was used to acquire and reconstruct images (retrospective method based on phase detection). All patients had an ITV defined using the maximum intensity projection (MIP). A PTV was created as a 5 mm isotropic expansion of the ITV.

Phantom

A motor driven moving phantom was customized with an add-on device consisting of a circular 3 cm diameter tissue equivalent sphere in polystyrene. The phantom moves in the cranio-caudal direction (2 cm peak-to-peak), with a frequency of 15 cycles/min and with an 'inspiration' phase shorter than the 'expiration' phase. EBT3 films can be inserted in the sphere simulating the target.

Plans were generated on the AVG CT in two different ways: 1) with no density override and 2) setting the ITV density to the mean GTV density and the PTV-ITV shell to an intermediate density between lung and GTV. The density override was performed with the further aim of reducing the dose distribution modulation that is induced by the difference in density between ITV and PTV-ITV, but which is neither intentional nor desired.

In order to single out the interplay effect, plans were also generated optimizing and prescribing to the ITV only (both with and without density override).

Average treatment time was 10 min (150 cycles per treatment).

Results:

Patients

In Table the results of the patient plan are reported, showing moderate variations between the AVG CT plan and the plans recalculated on each phase of the 4DCT. None of the parameters shows any statistically significant correlation between the variation and the extent of tumour displacement.

Patient	CT	ITV (cc)	GTV motion (cm)	PTV coverage (%)	Min PTV dose (Gy)	Mean PTV dose (Gy)	Max PTV dose (Gy)	Max lung dose (Gy)	Conformity Index (Paddick)	MCS
1	AVG	13,2	1,4	100,00	52,06	54,07	56,51	50,88	0,50	0,43
	Range on phases			94,09-99,21	50,61-51,35	53,04-53,69	51,30-56,01	49,99-50,73	0,26-0,46	
2	AVG	31,3	1,3	95,33	49,05	53,80	56,49	50,97	0,41	0,28
	Range on phases			92,90-96,57	48,45-49,52	53,45-54,09	56,64-57,67	50,77-51,24	0,35-0,47	
3	AVG	17	1,3	96,00	49,50	55,77	61,85	50,20	0,70	0,28
	Range on phases			95,32-96,81	49,19-49,65	55,38-55,73	61,69-62,21	49,79-50,20	0,64-0,70	
4	AVG	8,3	1,2	99,22	54,07	56,43	60,87	52,04	0,77	0,31
	Range on phases			90,71-98,14	52,95-53,75	55,63-56,06	58,63-58,88	51,31-51,73	0,80-0,84	
5	AVG	13,6	0,3	96,81	49,83	53,88	56,64	48,56	0,51	0,20
	Range on phases			93,62-95,84	49,54-50,08	53,40-53,64	56,26-56,41	48,00-48,38	0,27-0,43	
6	AVG	7,1	0,9	100,00	52,49	55,77	60,48	51,99	0,67	0,17
	Range on phases			99,13-99,92	51,36-52,46	55,02-55,90	59,87-60,79	51,12-52,02	0,59-0,66	
7	AVG	5,5	0,5	99,74	53,34	55,28	57,27	50,01	0,57	0,32
	Range on phases			99,73-100,00	51,85-52,74	54,40-54,98	56,85-57,39	48,94-49,85	0,45-0,53	
8	AVG	11,3	0,8	98,37	49,82	54,93	59,08	53,22	0,73	0,26
	Range on phases			97,60-98,16	48,30-49,34	54,10-54,77	58,17-59,10	52,31-53,29	0,50-0,63	
9	AVG	11,9	1,4	100,00	55,60	56,11	57,15	53,89	0,62	0,33
	Range on phases			99,99-100,00	53,09-54,40	55,75-55,89	57,13-57,84	53,40-53,71	0,62-0,66	
10	AVG	4,1	1,0	99,88	51,67	53,74	56,73	50,62	0,36	0,33
	Range on phases			91,27-99,52	50,51-51,42	52,98-53,62	56,14-56,48	49,64-50,63	0,25-0,38	
Mean variation (1SD)		13 (8)	1,0 (0,4)	1,3 (1,5)	0,58 (0,56)	0,33 (0,20)	0,44 (0,85)	0,35 (0,17)	0,4 (0,9)	0,29 (0,07)

Table. Parameters of the plan on the AVG CT and the corresponding range on all phases of the 4DCT. GTV motion values represent a 3D displacement of the tumour over the respiration cycle. The MCS is the Modulation Complexity Score which can be used for plan complexity evaluation (Masi et al., Med Phys 2013).

Phantom

When the dose verification is performed on moving phantoms, an average deterioration of the gamma passing rates of 20% is observed compared to the verification in static phantom. The plans optimized with densities override did not show an improved agreement between dose and calculation in moving phantom (Figure).

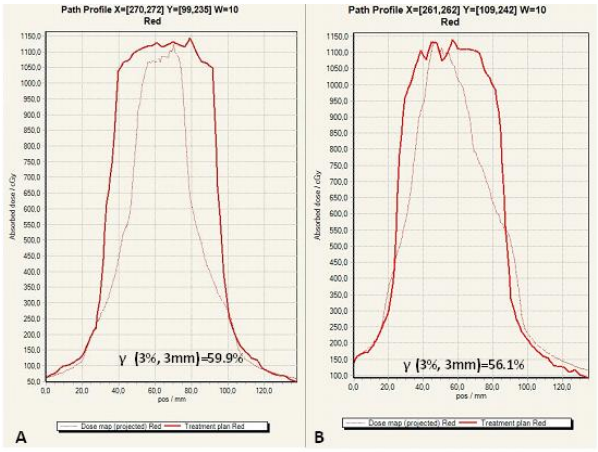

Figure. As an example, the cranio-caudal profiles at isocenter (comparison between measurement and calculation) are shown for the plans optimized on the ITV measured on moving phantom both without (A) and with (B) density override. The corresponding γ passing rates for the plans calculated and measured on the static phantom are 90.7% and 91.1% respectively.

Conclusions: The average CT is adequate for planning only as a first approximation, as significant interplay effects between the target motion and the intensity modulated dose delivery exist. The agreement between planned and measured dose distribution does not improve when density overrides in the ITV and PTV regions are applied.

PO-0950

Validation of the deformable image registration system elastix in the head and neck region

R. Zukauskaite[1], C. Brink[2], C.R. Hansen[3], A. Bertelsen[4], C. Grau[5], J. Johansen[1], J.G. Eriksen[1]

[1]Odense University Hospital, Department of Oncology, Odense, Denmark

[2]University of Southern Denmark, Institute of Clinical Research, Odense, Denmark

[3]University of Sydney School of Physics, Institute of Medical Physics, Sydney, Australia

[4]Odense University Hospital, Laboratory of Radiation Physics, Odense, Denmark

[5]Aarhus University Hospital, Department of Oncology, Aarhus, Denmark

Purpose/Objective: Deformable registrations of medical images are becoming widely used for both radiotherapy optimization, but also for treatment response evaluation, e.g. defining relapses. However, the accuracy of deformable image registration (DIR) is rarely validated. The current study evaluates the accuracy of the open source deformable registration tool *elastix* when used for registration of different organ structures on planning CT and relapse CT scans of head and neck patients.

Materials and Methods: Twenty patients treated with definitive IMRT for oral cavity, oropharynx and hypopharynx cancer in 2010-2012 were retrospectively and randomly included in the study. For each patient a planning CT and a diagnostic relapse CT scan were used (CT voxels were 3 mm in the cranio-caudal (CC) direction and 1 mm in the in-plane directions).

One observer manually contoured 8 organs (spinal cord, mandible, right/left parotid and submandibular glands, thyroid gland and vertebrae C3-5) on planning CT (pCT), relapse CT (rCT) and re-delineated again on the planning CT (reCT).

The contouring on the relapse CT was mapped to the planning CT using *elastix (*http://elastix.isi.uu.nl/*)*. Spatial analysis of the difference in ROI delineation was performed by measuring the minimum distance between the two ROI's on each surface point of the original ROI. For each ROI the combined uncertainty of DIR and delineation was calculated as the standard deviation of the minimum surface distances. Organ type specific uncertainties were calculated as Root-Mean-Square (RMS) of the patient individual standard deviations.

Re-delineation was used as a baseline for the obtainable uncertainty. Spearman's correlation between uncertainties of re-delineation and deformed delineation was performed to check whether delineation uncertainty influenced the outcome of the deformable results.

Results: Surface plot of the spatial resolved deviation showed that the largest deviations where mainly in the CC direction (areas where the ROI surface normal primarily is in the CC direction) (left submandibular gland as an example, picture). RMS values for re-delineation and DIR are shown in table.

A significant but low correlation exists between the ROI uncertainty of individual re-delineation and deformable contours (R=0.23, p=0.004). Thus a part of the deformable uncertainties are related to uncertainty of the manual ROI delineation. Significant correlations within single organs were not found.